JOURNAL OF MATERIALS SCIENCE 24 (1989) 4037–4041

The study of structural and electrical properties of thin antimony films

AJAY KUMAR, O. P. KATYAL
Department of Physics, Indian Institute of Technology, Kanpur 208 016, India

Structural and electrical properties of thin antimony films of various thicknesses evaporated on to glass substrates have been studied in the temperature range 150 to 350 K. The structural studies show that the films are polycrystalline having grains whose size increases with thickness. The electrical resistivity is found to increase as thickness decreases, thus exhibiting the size effect. The effect of grain-boundary scattering has been studied using a Mayadas–Shatzkes model and a three-dimensional model. The experimental results on the electrical resistivity are found to be consistent with the three-dimensional model. The specularity parameter $p \approx 0.49$, and has no temperature dependence. The values of reflection coefficient, R, and transmission coefficient, t, are determined from the experimental data.

1. Introduction

The electron transport properties of semimetal films have drawn the attention of many researchers in the past. The properties of a thin film of a material may differ from those of the bulk material in many ways, particularly if the film thickness is small. It has been predicted that a classical size effect will be revealed when the thickness of a film is comparable with the mean free path of the charge carriers in the film. Recently this classical size effect has been studied taking into account not only the external surface effects [1, 2] but also the presence of grain boundaries [3–12].

The study of electrical resistivity of semimetal films has mainly concerned the effects of grain boundaries and quantum size. Most investigations have been performed using bismuth films. Antimony has attracted less attention as a representative semimetal although it is one of the constituent materials of many binary and ternary compounds used in electron devices.

The electrical properties of antimony films have been studied by several authors [13–16]. Recently, Deschacht *et al.* [17] have studied the electrical properties of antimony films. They investigated the effect of grain boundary on the electrical resistivity, and also explained [18, 19] the experimental results on temperature coefficient of resistivity (TCR) and thermoelectric power (TEP) using a modified form of the Mayadas–Shatzkes (MS) expression.

The electrical resistivity of bismuth and antimony films deposited on to a glass substrate at a pressure of 10^{-10} torr was studied by Pariset [20]. He found that crystal size could be kept constant with increasing thickness by using appropriate heat treatments and an epitaxial technique. The experimental results were in good agreement with an approximate form of the size effect theories of Fuchs–Sondheimer [1, 2] (FS) and Mayadas–Shatzkes [3] (MS). De *et al.* [21] have reported measurements of the electrical resistivity, TCR, Hall coefficient and TEP of antimony films *in situ*. They observed that the M–S equation with specularity parameter $p = 0$ and grain-boundary reflection coefficient $R = 0.15$ reproduced the experimental results. The structural and galvanomagnetic properties of thin antimony films deposited at various substrate temperatures were studied by Mojejko–Kotlinska and Subotowicz [22]. They analysed the results on the basis of FS and M–S theories. The aim of the present work is to study the electrical conduction in thin antimony films at different temperatures. The experimental observations have been correlated with the structure of the films and the results have been explained using the MS model [3] and three-dimensional model of Pichard *et al.* [9, 11, 23, 24].

2. Experimental details

Cleaned glass slides were used to deposit four silver (99.99%) electrodes over which antimony (99.999%) was deposited by thermal evaporation in a vacuum better than 10^{-5} torr. During evaporation, the substrate temperature was kept at 350 K for all the samples. The evaporation rate was fixed at $\approx 1\ \mathrm{nm\,sec^{-1}}$. During deposition, the thickness was controlled by a quartz crystal monitor and it was measured using an optical method. A constant current of a few milliamps was passed through the outer electrodes and the potential drop was measured across the inner two electrodes using a K-3 potentiometer. The current through the sample was estimated by measuring the potential drop across a standard resistance. Measurements of electrical resistance were carried out *in situ*. The temperature of the substrate was varied using a cold finger, filled with liquid nitrogen and fitted with a heater at the bottom near the substrate. The temperature was measured using a copper–constantan thermocouple placed on the substrate.

0022-2461/89 $03.00 + .12

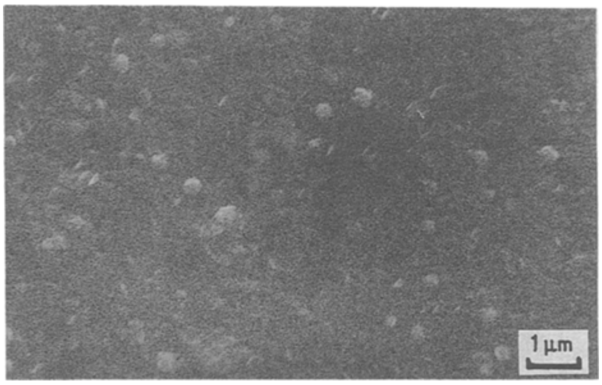

Figure 1 Scanning electron micrograph of antimony film of thickness 335.5 nm.

2.1. Structural studies

The structure of the antimony films was studied using a scanning electron microscope (Jeol JSM-35 C.F) and an X-ray diffractometer (Iso-Debyeflex 2002D). The effective grain size, D, was determined from the diffraction peaks (see Fig. 2) by using the equation

$$D = \frac{\lambda}{B_c \cos\theta} \tag{1}$$

where λ is the X-ray wavelength, θ is the Bragg angle and B_c is the true width of diffraction peak at half of the maximum intensity. The average grain size was also measured from the micrographs (Fig. 1). These two methods gave approximately the same results.

These studies show that films are polycrystalline and their grain size increases with the thickness. The films are strongly textured as evidenced by strong (0003), (0006) and (0009) reflections (Fig. 2).

3. Results and discussion

Fig. 3 shows the temperature dependence of resistivity for the antimony films of different thicknesses. The first analysis of electrical measurements data for thin films was carried out by Fuchs [1] and Sondheimer [2], who proceeded from the solution of the Boltzmann equation. Generally, to compare experimental data with the theoretical predictions of the FS model, it is usually to fit data with the limiting form of resistivity

$$\varrho_F = \varrho_\infty\left[1 + \tfrac{3}{8}\, l_\infty \frac{(1-p)}{d}\right] \tag{2}$$

where ϱ_∞ and l_∞ are, respectively, the resistivity and mean free path of the bulk material having the same defect density as that of the film, d is the film thickness and p is the specularity parameter. Equation 2 indicates a linear dependence of resistivity on $(\text{thickness})^{-1}$. The measured film resistivity (ϱ_F) at different temperatures is plotted as a function of $1/d$ in Fig. 4. These variations are found to be linear. The bulk resistivity can be obtained from the intercept of the corresponding plot, while the slope of the curve in Fig. 4 will give the value of $\frac{3}{8}\varrho_\infty l_\infty(1-p)$. The values of ϱ_∞ obtained here are very close to the pure bulk resistivity, ϱ_0, and this difference remains approximately constant at the other temperatures. Knowing the value of ϱ_∞ and $l_\infty(1-p)$, it remains to determine the value of the specularity parameter p. For this, first we evaluate the value of mean free path, l_∞, using the relation $\varrho_0 l_0 = \text{constant}$ [20]. In Fig. 4 slope of the curves remains constant, which indicates that the specularity parameter, p, has no temperature dependence. The calculated values of ϱ_∞, $l_\infty(1-p)$, p, etc., at temperatures 150, 225 and 300 K are given in Table I. For comparison, the results of other researchers are also included in that Table. Bulk parameters are taken from the paper of Oktu and Saunders [25].

Fuchs model is not appropriate to explain our results on the resistivity of the antimony films, because it reproduces the results only in the high thickness region and deviates appreciably in the low thickness region, but the value of bulk resistivity can be found be applying Fuchs model.

The resistivity of a polycrystalline film has a contribution of resistivity due to scattering of conduction electrons from phonons and defects, from film surface and from grain boundaries. To consider the effect of grain-boundary scattering on the transport properties of metal films, Mayadas and Shatzkes presented a model in which, for a polycrystalline film of thickness d, the total resistivity ϱ_F including isotropic back-

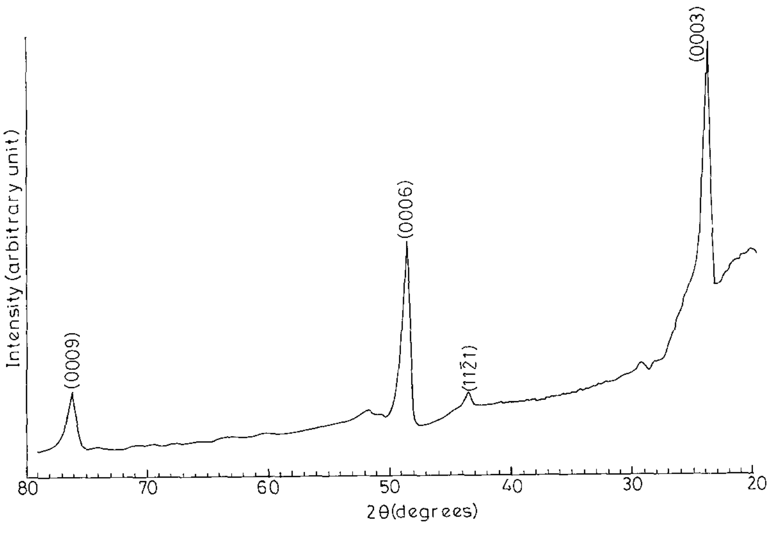

Figure 2 X-ray diffractogram of antimony film of thickness 335.5 nm.

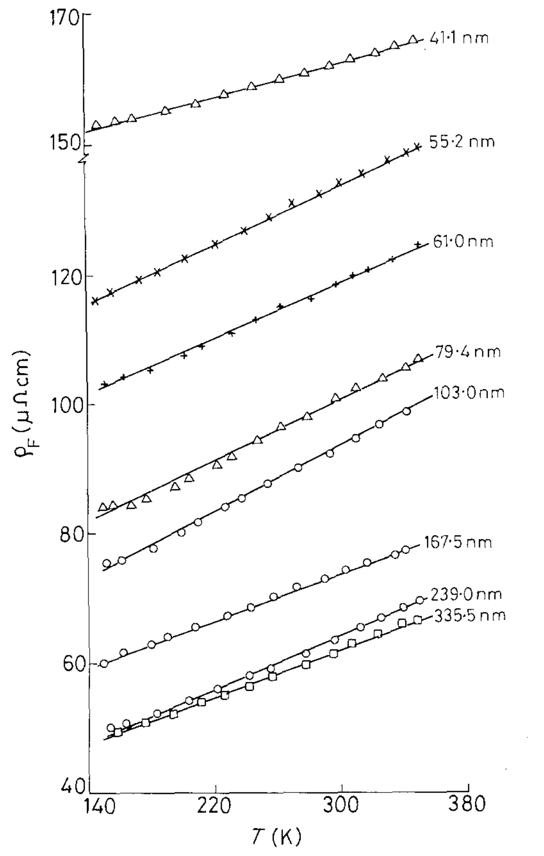

Figure 3 Temperature dependence of resistivity for antimony films.

ground scattering, grain-boundary scattering and external surface scattering, is given as [3]

$$\frac{\varrho_F}{\varrho_g} = \left[1 - \frac{A}{f(\alpha)}\right]^{-1} \tag{3}$$

where

$$A = \frac{6}{\pi k}(1 - p)\int_0^{\pi/2} d\Phi \int_1^{\infty} \frac{\cos^2\Phi}{H^2(t_1, \Phi)}\left[\frac{1}{t_1^3} - \frac{1}{t_1^5}\right] \times \frac{1 - \exp[-kt_1 H(t_1, \Phi)]}{1 - p\exp[-kt_1 H(t_1, \Phi)]}\, dt_1 \tag{4}$$

with

$$H(t_1, \Phi) = 1 + \alpha(\cos\Phi)^{-1}\left[1 - \frac{1}{t_1^2}\right]^{-1/2}$$

ϱ_g, which represents the resistivity due to both isotropic background scattering and grain-boundary scattering, is connected to bulk resistivity, ϱ_0, by the relation

$$\frac{\varrho_0}{\varrho_g} = f(\alpha) = 1 - \tfrac{3}{2}\alpha + 3\alpha^2 - 3\alpha^3 \ln(1 + \alpha^{-1}) \tag{5}$$

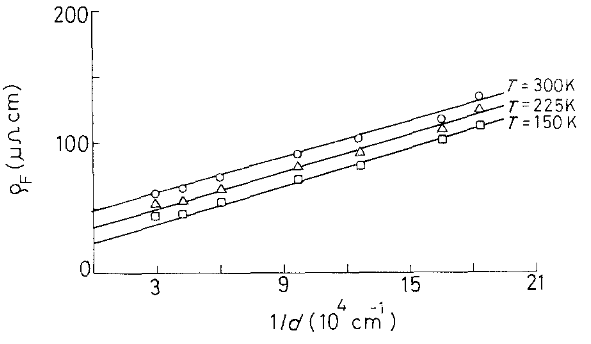

Figure 4 Plot of film resistivity (ϱ_F) against inverse of thickness (d^{-1}).

and

$$\alpha = \frac{l_0 R}{D(1 - R)} \tag{6}$$

where R is the reflection coefficient at the grain boundary, l_0 the bulk mean free path, D the average grain diameter and k the reduced thickness; Φ and t_1 are the integration variables. Equation 4 is complicated, and cannot be evaluated analytically, and for comparison with the experiments, numerical solutions are necessary. Several approximations have been derived from the MS model for comparison with the experimental results [4, 5].

Another model which considers the effect of grain-boundary scattering on the electrical resistivity of film, was proposed by Pichard *et al.* [9] (PTT). It is a three-dimensional model, in which it is assumed that grain boundaries in polycrystalline films can be represented by three arrays of mutually perpendicular planar potentials. The average effect of a grain-boundary is represented by a specular transmission coefficient, t, which gives the fraction of electrons whose velocity in the electric field direction is not altered by the grain boundary, whereas the remainder of the electrons are diffusely scattered and do not contribute to the current [9, 11]. Assuming that the probability of an electron travelling a given distance, without being diffusely scattered, is given by an exponential law [11], a mean free path can be ascribed to the three-dimension array of scatterers whose spacing is identified with average grain diameter D. They further introduced a parameter v, known as the grain-boundary parameter, defined as [9]

$$v = \frac{D}{l_0}\left[\ln\left(\frac{1}{t}\right)\right]^{-1} \tag{7}$$

The ratio of an infinitely thick polycrystalline film

TABLE I

T_s (K)	Temp. (K)	ϱ_0 ($\mu\Omega$ cm) Bulk	l_0 (nm) Bulk	ϱ_∞ ($\mu\Omega$ cm)	$l_\infty(1 - p)$ (nm)	p	R	t	Reference
350	150			22.00	538.6	0.49	0.176	0.820	present study
	225	31.5	335.0	35.00	338.6	0.49	0.150	0.845	
	300	46.0	230.0	49.00	241.8	0.48	0.115	0.877	
333 to 383	293	-	-	55.00	300.0	0.15	0.24		Kotlinska *et al.* [22]
	300	-	-	52 to 63*	50 to 55*	0.75 to 0.68*			Pariset [20]
423	300	-	-	70.00	51.0	0	0.15		Pal *et al.* [21]

*Depending on preparation conditions.

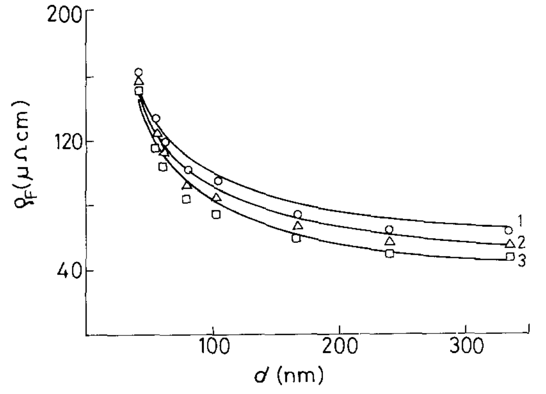

Figure 5 Electrical resistivity plotted against thickness of antimony films. (——) Equation 10. Curves: (1) $p = 0.48$, $t = 0.877$, (○) experimental points at 300 K; (2) $p = 0.49$, $t = 0.845$, (△) experimental points at 225 K; (3) $p = 0.49$, $t = 0.820$, (□) experimental points at 150 K.

conductivity to the bulk material was found to be [9, 26]

$$\frac{\sigma_g}{\sigma_0} = \frac{\varrho_0}{\varrho_g} = \frac{3}{2}\frac{\nu}{1 - C} \times [\gamma - \tfrac{1}{2} + (1 - \gamma^2)\ln(1 + \gamma^{-1})] \tag{8}$$

with

$$\gamma = \frac{\nu + C^2}{1 - C}; \quad C = \frac{4}{\pi}$$

With the consideration of partially diffuse scattering, the external size effect can be analysed in terms of Cottey's model [27] in which a mean free path is associated with scattering; an external surface parameter, μ, can be introduced to describe the size effect, i.e.

$$\mu = \frac{d}{l_0}\left(\ln\frac{1}{p}\right)^{-1} \tag{9}$$

Consequently, in thin polycrystalline films in which three types of electron scatterings (background, grain-boundary and external surface scattering) are simultaneously operative, the electrical conductivity, σ_F, takes the simple analytical form [23, 24]

$$\frac{\sigma_F}{\sigma_0} = \frac{3}{2}\frac{1}{b}[a - \tfrac{1}{2} + (1 - a^2)\ln(1 + a^{-1})] \tag{10}$$

with

$$b = \mu^{-1} + \nu^{-1}(1 - C) \tag{11}$$

$$a = (1 + C^2\nu^{-1})b^{-1} \tag{12}$$

Recently, it has been shown [28, 29] that whatever the film structure, Equation 10 can be used for describing the electrical conductivity of the film (σ_F). Pichard *et al.* [9] have also shown that the MS model and the three-dimensional grain-boundary model are very similar.

Estimating the contribution to the resistivity due to the surface from

$$\varrho_s = \frac{3}{8}\frac{\varrho_\infty l_\infty(1 - p)}{d} \tag{13}$$

with the determined value of p and attributing the difference to the grain boundaries, we have calculated the experimental values of grain-boundary resistivity ϱ_g. The MS Equation 5 with $R = 0.115$ and Equation 8 of the three-dimensional model with $t = 0.877$ at 300 K reproduces the experimental results on grain boundary resistivity. The experimental results on ϱ_g and theoretical values at 150, 225 and 300 K are given in Table II. From Table II we see that there is a reasonably good fit between theoretical and experimental results and both models (MS and PTT) give almost the same results. Therefore, as already mentioned [23], Equation 10 can be used as an alternative formulation for the complicated expression of total film conductivity (Equation 3) obtained in the MS model. For various calculations from these equations, we have used a DEC 10 Computer. With $t = 0.877$, $p = 0.48$, $\varrho_\infty = 49\,\mu\Omega$ cm and $l_\infty = 215$ nm (at 300 K), Equation 10 reproduces the experimental results on total film resistivity. Fig. 5 shows that there is a good agreement between the experimental results and theoretical variations of Equation 10 at 150, 225 and 300 K.

4. Conclusions

The polycrystalline antimony film deposited on to glass substrates exhibit a size effect. The experimental results on the resistivity can be successfully explained by a simple analytical equation of a three-dimensional model. The specularity parameter $p = 0.49$, and is temperature independent. The value of R is about 0.115 to 0.176 while the value of t is about 0.820 to

TABLE II

d (nm)	D (nm)	$T = 300$ K, $p = 0.48$			$T = 225$ K, $p = 0.49$			$T = 150$ K, $p = 0.49$		
		$\left(\frac{\varrho_0}{\varrho_g}\right)_{exp}$	$\left(\frac{\varrho_0}{\varrho_g}\right)_{PTT}$ $t = 0.877$	$\left(\frac{\varrho_0}{\varrho_g}\right)_{MS}$ $R = 0.115$	$\left(\frac{\varrho_0}{\varrho_g}\right)_{exp}$	$\left(\frac{\varrho_0}{\varrho_g}\right)_{PTT}$ $t = 0.845$	$\left(\frac{\varrho_0}{\varrho_g}\right)_{MS}$ $R = 0.150$	$\left(\frac{\varrho_0}{\varrho_g}\right)_{exp}$	$\left(\frac{\varrho_0}{\varrho_g}\right)_{PTT}$ $t = 0.820$	$\left(\frac{\varrho_0}{\varrho_g}\right)_{MS}$ $R = 0.176$
41.1	47.5	0.435	0.526	0.544	0.323	0.382	0.385	0.211	0.240	0.241
55.2	59.8	0.506	0.583	0.604	0.395	0.437	0.446	0.277	0.292	0.296
61.0	67.6	0.581	0.612	0.628	0.452	0.468	0.480	0.315	0.318	0.326
79.4	75.1	0.650	0.637	0.655	0.529	0.494	0.504	0.379	0.341	0.350
103.0	87.5	0.662	0.671	0.688	0.543	0.532	0.553	0.401	0.377	0.387
167.5	125.6	0.793	0.746	0.758	0.636	0.620	0.626	0.454	0.464	0.469
239.0	176.0	0.884	0.804	0.814	0.724	0.696	0.700	0.546	0.548	0.551
335.5	234.2	0.871	0.845	0.852	0.711	0.752	0.756	0.521	0.617	0.618

0.877. The comparatively large dispersion of mean free path values reported by various workers (Tabel I) is probably due to the different experimental conditions used during the deposition of films.

Acknowledgements

The authors thank the Defence Electron Microscope Laboratory (DMSRDE, Kanpur), and especially Dr P. T. Rajagopalan for help with the electron micrographs.

References

1. K. FUCHS, *Proc. Camb. Phil. Soc.* **34** (1938) 100.
2. E. H. SONDHEIMER, *Adv. Phys.* **1** (1952) 1.
3. A. F. MAYADAS and M. SHATZKES, *Phys. Rev. B* **1** (1970) 1382.
4. G. WEDLER and P. WISSMANN, *Ber. Bunsenges. Phys. Chem.* **74** (1970) 934.
5. E. E. MOLA and J. M. HERAS, *Thin Solid Films* **18** (1973) 137.
6. F. THIEME and W. KIRSTEIN, *ibid.* **30** (1975) 371.
7. F. WARKUSZ, *Acta. Phys. Pol. A* **54** (1978) 31.
8. F. WARKUSZ, Report 159180 Technical University Warsaw (1980).
9. C. R. PICHARD, C. R. TELLIER and A. J. TOSSER, *Thin Solid Films* **62** (1979) 189.
10. C. R. TELLIER and A. J. TOSSER, *ibid.* **70** (1980) 225.
11. C. R. TELLIER, C. R. PICHARD and A. J. TOSSER, *ibid.* **61** (1979) 349.
12. C. R. PICHARD, YU. F. KOMNIK, B. I. BELEVTSEV and A. J. TOSSER, *J. Mater. Sci. Lett.* **2** (1983) 360.
13. KUNISUKE MAKI, *Jpn J. Appl. Phys.* **12** (1973) 146.
14. A.COLOMBANI, C. VAUTIER and P. HUET, *C.R. Acad. Sci.* **21** (1958) 1838.
15. D. C. BARUA and K. B. BARUA, *Ind. J. Phys.* **49** (1975) 603.
16. K. PAPROCKI, K. MOJEJKO, M. SUBOTOWICZ and M. JALOCHOWSKI, *Thin Solid Films* **36** (1976) 93.
17. D. DESCHACHT, A. BOYER and E. GROUBERT, *ibid.* **70** (1980) 311.
18. A. BOYER, D. DESCHACHT and E. GROUBERT, *ibid.* **76** (1981) 119.
19. D. DESCHACHT and A. BOYER, *J. Mater. Sci.* **20** (1985) 807.
20. C. PARISET, *Thin Solid Films* **91** (1982) 301.
21. D. DE, C. K. GHOSH and A. K. PAL, *ibid.* **110** (1983) 193.
22. K. MOJEJKO-KOTLINSKA and M. SUBOTOWICZ, *ibid.* **111** (1984) 235.
23. C. R. PICHARD, C. R. TELLIER and A. J. TOSSER, *J. Mater. Sci.* **15** (1980) 2236.
24. C. R. TELLIER and A. J. TOSSER, "Size Effects in Thin Films", (Elsevier, Amsterdam, New York, 1982) Ch. 1.
25. O. OKTU and G. A. SAUNDERS, *Proc. Phys. Soc.* **91** (1967) 156.
26. C. R. PICHARD, C. R. TELLIER and A. J. TOSSER, *Phys. Status Solidi (a)* **65** (1981) 327.
27. A. A. COTTEY, *Thin Solid Films* **4** (1968) 297.
28. M. BEDDA, S. MESSAADI, C. R. PICHARD and A. J. TOSSER, *J. Mater. Sci.* **21** (1986) 2643.
29. C. R. PICHARD, V. I. VATAMANYUK, A. KHALID-NACIRI, C. R. TELLIER and A. J. TOSSER, *J. Mater. Sci. Lett.* **3** (1984) 447.

Received 21 July 1988
and accepted 31 January 1989